Modeling the Multidimensional Approach of Uncertainty in Environmental Measurements: Nanoinstrumentation Issues

A. Lay-Ekuakille, G.Griffo and P. Vergallo
Department of Innovation Engineering, University of Salento, 73100 Lecce, Italy
Email: aime.lay.ekuakille@unisalento.it

***Abstract*—Nanotechnology is an opportunity for environmental measurements. If we consider an environmental matrix like a biological material, it is possible to investigate on it using non invasive technique and applying certain techniques as beamforming. The main idea of the work is to detect, thanks to acoustic waves, metallic materials or plastic ones included in a confined ambient and that are contaminated. There are different sensor techniques based on micro and nanotechnology for investigating on environmental issues. The purpose of this paper is to illustrate an overview and application of processing signal from acoustic nanosensors for localizing materials inside others. A modeling of accuracy, hence uncertainty, is outlined.**

***Index Terms*—Environmental measurements, nanosensing, nanoinstrumentation, multidimensional approach of uncertainty, beamforming, acoustic sensing and detection, distribution**

I. Introduction

The detection of hazardous materials for environmental monitoring and protection is a matter of high interest world wide. Monitoring material encapsulated in another matrix is also a challenging activity because we shall identify hidden materials of interest. There are many significant apparatuses able to perform this kind of duty. Most of them are very big and the interest of current research is to develop small devices to be used as portable system for a quick but more precise analysis. Moreover the retrieval of polluted/contaminated material which is confined in other structure can be done using nanotechnology, especially nanosensors.

However, each detecting system based on sensors must have some essential requirements that are illustrated in Table I. The above requirements are regardless of the transducing mechanism (electrical, optical, mass, thermal, piezoelectric, etc.), the recognition principle (enzymatic, DNA, molecular recognition, etc.) or the applications (environmental, food, medical diagnosis, etc.). There is a big number of nanosensors for the envisaged applications, for example: piezoelectric cantilever sensors (PECS) with a nonpiezoelectric extension, sensors based on nanoparticles and nanoclusters, sensors based on nanowires and nanotubes, sensors based on nanostructures embedded in bulk material, sensors based on porous silicon, nanomechanical sensors, self-assembled nanostructures, receptor-ligand nanoarrays, [2], [3] etc... We want to focus on introductory aspects of nanopiezoelectric sensors.

Performance parameter	Definition
Sensitivity	The slope of a calibration curve or change in unit sensor response with change in unit analyte concentration
Limit of detection (LOD)	Lowest analyte concentration value that can be detected
Resolution	Smallest concentration variation that can be detected when the concentration is continuously changed
Dynamic range	The analyte concentration from LOD to maximum concentration that can be reliable detected
Selectivity	The ability to detect a specific analyte in the presence of other molecules
Reversibility	The ability of the sensor to return back to its original value when the analyte is removed
Response time	The time required to respond from zero analyte concentration to a step in the concentration
Linearity	The range where the sensor response is in direct proportion to the analyte concentration
Hysteresis	The difference in sensor characteristics for increasing and decreasing analyte concentrations

TABLE I
Influence on human health

Having nanosensor modeling a high resolution in space and in time, it is basically important to generate numerically accurate simulations of electromagnetic wave interactions. It is quite common to design dielectric devices embodying nanoparticles, quantum dots, nanorods or other nano discontinuities. The interest is in simulating at nanometer resolution the behavior of these devices with an overall size of tens or hundreds of nanometers. In particular the critical configurations where the accuracy could fail at optical frequencies are: nanodefects, high bulk dimension in bulk-type structures, nanostructures in long optical fiber, singularity points, very thin dielectric layer in very long dielectric structure, dielectric discontinuities. Traditional numerical methods such as the Finite Element Method (FEM), the Beam Propagation Method (BPM), and the widely used FDTD (Finite Difference Time Domain) by Yee [4], require huge computational power to achieve the required level of accuracy of the electromagnetic

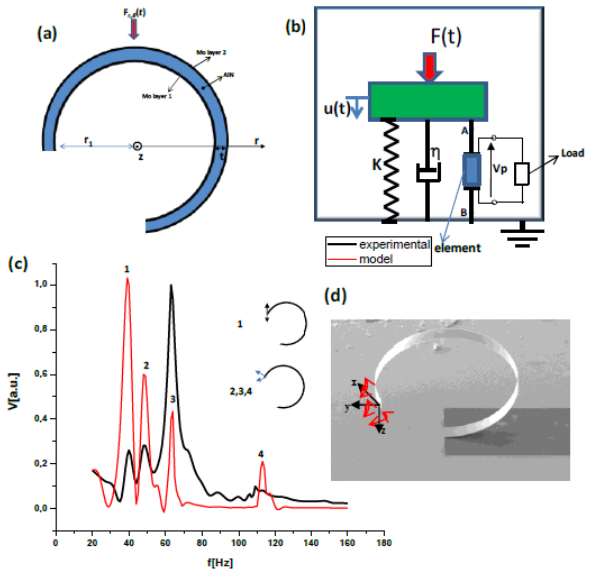

Fig. 1. (a) Coordinate system used in the R (ring) MEMS modeling. (b) Equivalent electromechanical model for vibrating energy harvesting cantilever system with proof mass. The losses are modelled by the mechanical resistance indicated by η. (c) Comparison between analytical and experimental voltage signal versus the frequency. Inset: configuration of the first main four modes. (d) Coordinate system indicating the possible movement of the RMEMS due to a vibrational force

solution.

Concerning a piezoelectric cantilever MEMS, a complete electromechanical model is illustrated in Fig. 1 (a), where a transduction system is enclosed in a package. The mechanical deformation of the cantilever device leads to an electrical signal using the piezoelectric effect: the external force F(t) shakes the cantilever beam along the vertical direction, the vibration, indicated by the function u(t), will generate through the piezoelectric effect a voltage Vp / current i signal at the output of the system. The system will be matched with an external load Z in order to transfer the maximum energy (see scheme of Fig. 1 (b)). A piezoelectric cantilever beam material (see example in Fig. 2 (b) where two metallic Molybdenum layers enclose the piezoelectric AlN layer) is proposed [5]. The layer thickness of the first metallic layer provides the strain properties of the whole free standing structure where two metallic layers (layer) enclose the piezoelectric AlN layer.

The layer thickness of the first metallic layer provides the strain properties of the whole free standing structure) will convert energy between the mechanical and electrical domains through the following relationships between the stress **T**, the strain **S**, the electric **E**, and the electric displacement field **D**

$$\begin{aligned} \mathbf{T} &= c_E\mathbf{S} - e^T\mathbf{D} \\ \mathbf{D} &= e\mathbf{S} - \epsilon_r\mathbf{E} \end{aligned} \tag{1}$$

where c_E, e, and ϵ_r are the elasticity matrix, the coupling matrix and the relative permittivity matrix, respectively,

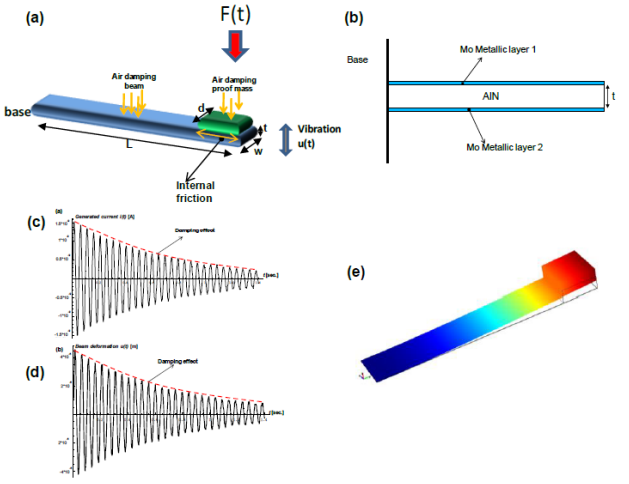

Fig. 2. (a) Losses of the piezoelectric cantilever element: damping mechanisms and internal friction of a cantilever in air. (b) Cross section of a complete cantilever AlN structure. (c) time domain current generated by the external force, and, (d) time domain beam deformation. (e) Cantilever deformation measure by FEM.

defined for the AlN material as

$$c_E = \begin{pmatrix} 4.1e^{11} & 1.49e^{11} & 9.9e^{10} & 0 & 0 & 0 \\ 1.49e^{11} & 4.1e^{11} & 1.49e^{11} & 0 & 0 & 0 \\ 9.9e^{10} & 1.49e^{11} & 3.89e^{11} & 0 & 0 & 0 \\ 0 & 0 & 0 & 1.25e^{11} & 0 & 0 \\ 0 & 0 & 0 & 0 & 1.25e^{11} & 0 \\ 0 & 0 & 0 & 0 & 0 & 1.25e^{11} \end{pmatrix} [Pa] \tag{2}$$

$$e = \begin{pmatrix} 0 & 0 & 0 & 0 & -0.48 & 0 \\ 0 & 0 & 0 & -0.48 & 0 & 0 \\ -0.58 & -0.58 & & 1.55 & 0 & 0 \quad 0 \end{pmatrix} [C/m^2] \tag{3}$$

$$\epsilon_r = \begin{pmatrix} 9 & 0 & 0 \\ 0 & 9 & 0 \\ 0 & 0 & 9 \end{pmatrix} [C/m^2] \tag{4}$$

The piezoelectric element is subjected to vertical mechanical vibration u(t) of the seismic mass (proof mass). This displacement is solution of the electromechanical system of equations.

II. Beamforming Aspects

Consider an array of sensors or 'Smart Antenna' collecting spatial samples of propagating wave fields. Signals may be present from any given direction and always in the presence of noise. The desired signal is from a particular spatial location. From a signal processing perspective, the main objective is to detect the signal arriving from a particular look direction and cancel out any interfering signals and noise. A beamforming processor can achieve this by electrically steering the Smart

Antenna, rather than mechanically as done in years gone by. The advantages of beamforming are improvements in communication quality, throughput and efficiency and as a result, have applications in fields such as radar, sonar, seismology and wireless communications.

A sensor array receives incoming signal information. A beamformer processes the spatial samples collected to provide the required spatial filtering [6]. The sensor array may be arranged in a number of different configurations, two of which are the Uniform Linear Array (ULA) and Uniform Circular Array (UCA) in 2D space. The beamformer linearly combines the spatially sampled time series from each sensor to obtain a scalar output time series. Beamformers are grouped into three different classes, fixed, optimum and adaptive. Fixed beamformers are analogous to bandpass filters, they strive to pass spatially signals from a desired look direction and suppress all other signals arriving from all other angles.

Furthermore, for practical purposes, interfering signals and noise are to be suppressed relative to the look direction. Suppose an antenna array receives N narrowband signals, s1(t), s2(t)....sN(t), each arriving from a distinct look direction θ1, θ2...θN the array output vector is given by

$$x(t) = a(\theta)s(t) + n(t) \tag{5}$$

where $n(t) = [n_1(t)n_2(t)...n_n(t)]^T$ is the noise output of the nth sensor. n(t) and s(t) are assumed to be stationary, zero mean and uncorrelated with each other. Also incoming signals are to hold the narrowband condition. The beamformer output is formed by applying a complex weights vector, w, to the N incoming signals received from the antenna array and summing the result, as shown in Fig 3. The beamformer output, y(t) to a signal approaching from direction is expressed as

$$\begin{aligned} y(t) &= w^H x(t) \\ w &= [w_1 w_2 ... w_N]^T \end{aligned} \tag{6}$$

where $x(t) = [x_1(t)x_2(t)...x_N(t)]^T$ where x(t) is defined according to Eq.(5) as a function of the received signal and the steering vector a(θ). The power response, F of the beamformer is defined as

$$F = |y(t)|^2 \tag{7}$$

Practical use of a beamformer processor usually requires real time operation and the main parameters of the beampattern are illustrated in Fig.4 which is a cross section of 3D representation [7].

The beampattern represents the energy distribution in the space during transmission and the direction of great and small sensitivity during receiving process [8].

III. Multidimensional Analysis and Modeling

The representation of back sensed signals thanks to beamforming illustrates the spatial trend of a special distribution

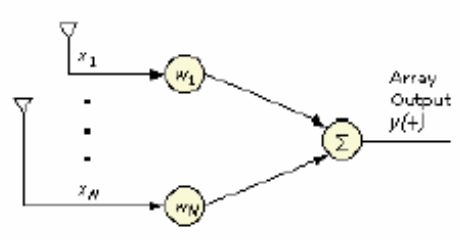

Fig. 3. Beamforming block diagram

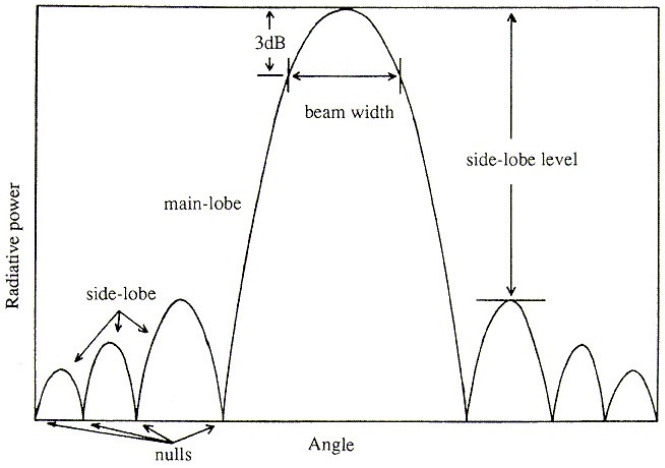

Fig. 4. Beamforming main parameter in terms of beampattern

similar to a copula. A copula help to separate the effect of dependence from the effect of marginal distributions in a joint distribution. Beamforming effects display a joint distribution of different signals with their direction of arrival (DOA) [9] related to sensors or nanosensors. A copula [10] is a distribution of the unit square with uniform marginal distributions. A copula can also be considered as distribution on [-1/2, 1/2]^2 with uniform margins on [-1/2, 1/2]. This kind of operation makes simple computation since then variables have means zero. Hence, copulae are functions that join or "couple" bivariate distribution functions to their marginal distribution functions.

Let us take into consideration Z as an absolutely continuous with density G(z) for z$\in$[0,1]. The density function of the generalized diagonal band copula is

$$bg(u,v) = \frac{1}{2}[G(|u-v|) + G(1-|1-u-v|)] \tag{8}$$

for $0 < u, y < 1$

This equation expresses the generalized diagonal band copula and is illustrated in Fig. 4.

As we have seen in previous section, the spatial representation of beamformed information is similar to Fig. 4. But in other circumstances using other kinds of beamformers [11]. In this we can obtain an elliptical copula as described in Fig. 6.

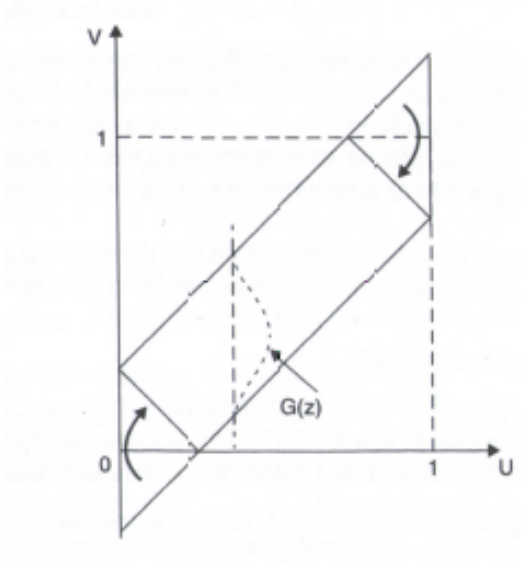

Fig. 4. Generalized diagonal band copula.

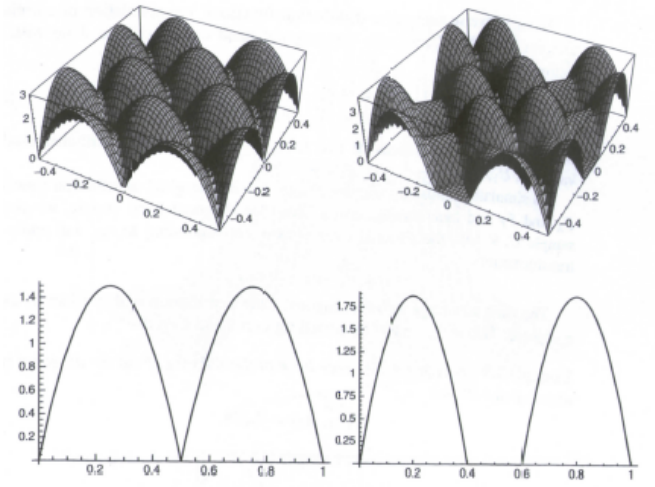

Fig. 5. Density functions of the generalized diagonal copulae. The distributions are below each density.

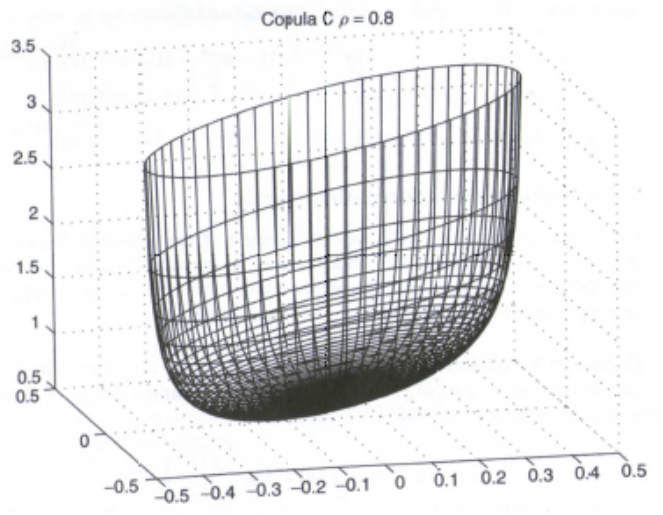

Fig. 6. Density function of an elliptical copula.

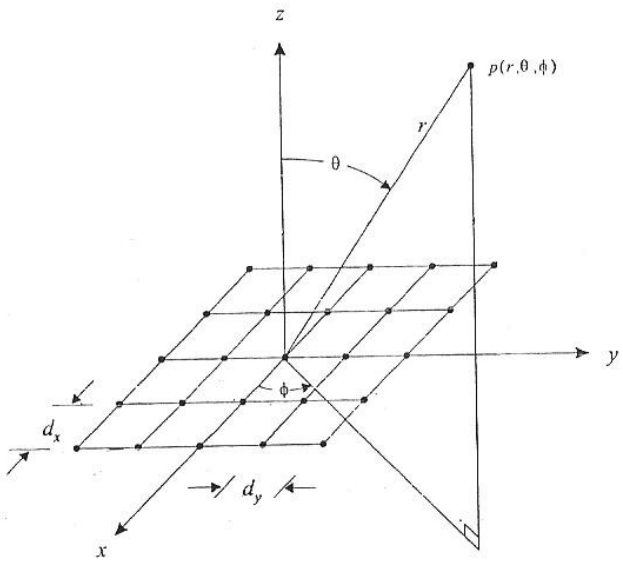

Fig. 7. Functional block diagram of the NE555 and amplitude vs pulse

IV. Presentation of Preliminary Results

We start with a simulation of an array of 5x5 sensors/nanosensors as graphically represented in Fig. 7. We use Esprit algorithm [12] in order to see the output for the following DOAs

- D ($\theta 1$, $\varphi 1$) = (40, 10) [SN R = 15dB]
- D ($\theta 2$, $\varphi 2$) = (70, 30) [SN R = 15dB]
- D ($\theta 3$, $\varphi 3$) = (80, 50) [SN R = 15dB]

We calculate the azimuths of all directions of arrival using Esprit algorithm as it results from Fig.8. After that we are able to compute the accuracy along azimuth direction. The Fig.9 and Fig.10 depict the 1D and 3D beampattern for the envisaged DOA respectively. Fig.9 displays the position of two hidden objects if they are encapsulated in an environmental matrix. The 3D representation is similar to the copula distribution we have seen in previous section and it is related to Fig.4. However, the proposed example is for an acoustic detection but it can used for any other radiation with specific assumptions.

References

[1] L. Senesac, T. G. Thundat, *Nanosensors for trace explosive detection*, Materialstoday, vol.11, n.3, pp.28-36, 2008.

[2] W.Y. Shih, W.H. Shih, *Nanosensors for Environmental Applications*, in Nanotechnologies for the Life Sciences, Wiley, 2007.

[3] J. Riu, A. Maroto, F. X. Rius, *Nanosensors in Environmental Analysis*, Talanta, vol.69, pp.288-301, 2006.

[4] K.S. Yee, J.S. Chen, *The finite-difference time-domain (FDTD) and the finite-volume time-domain (FVTD) methods in solving Maxwell's equations*, IEEE Transactions on Antennas and Propagation, vol.45, n.3, pp.354-363, 1997.

[5] A. Lay-Ekuakille, *Optical Waveguiding and Applied Photonics: Technological Aspects, Experimental Issue Approaches and Measurements*, Springer, 2013.

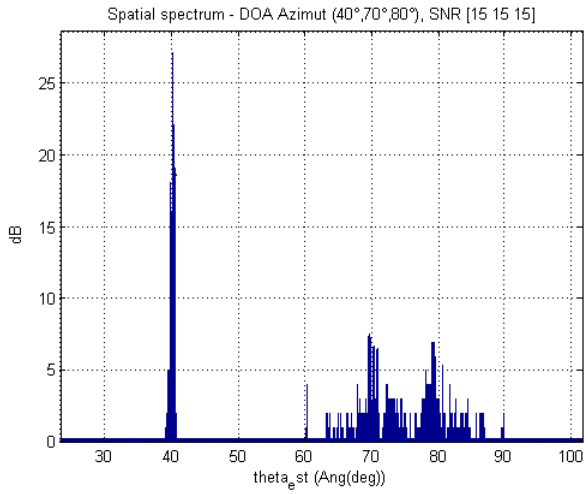

Fig. 8. Spatial spectrum of azimuths using Esprit algorithm.

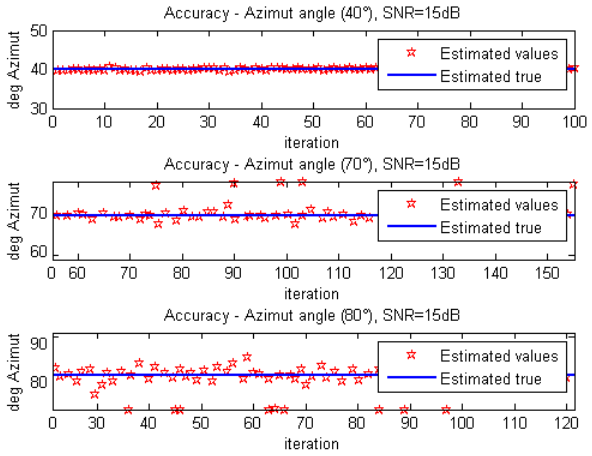

Fig. 9. Accuracy estimation in azimuths using Esprit algorithm.

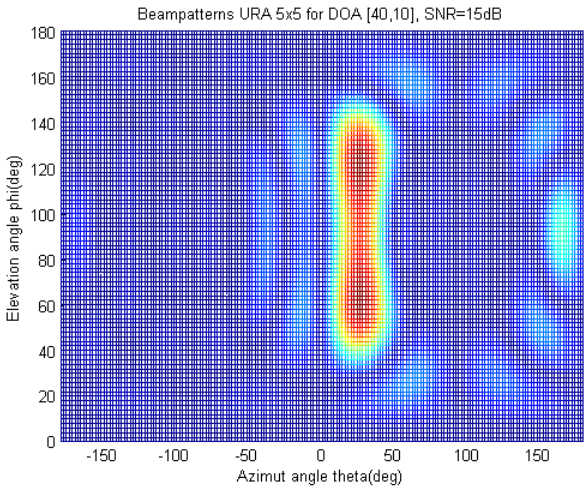

Fig. 10. Beampattern for DOA [40,10]]

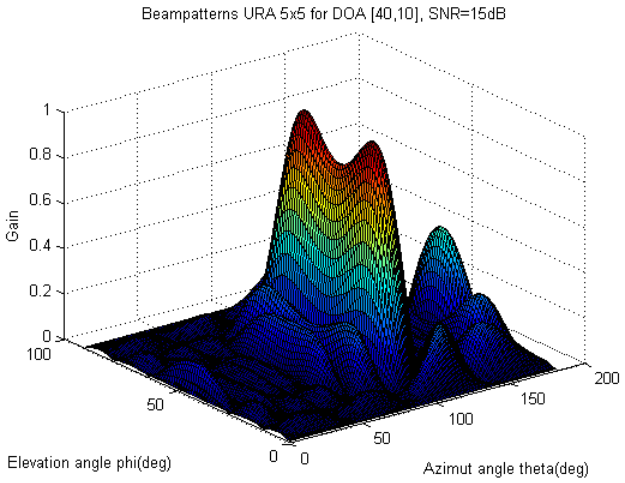

Fig. 11. 3D Beampattern for DOA [40,10]]

[6] K.L.Bell, H.L. Van Trees, *Adaptive Beamforming for Spatially Spread Sources*. In: Proc. Ninth IEEE SP Workshop on Statistical Signal and Array Processing, 1998, USA.

[7] A. Lay-Ekuakille, G. Vendramin, A. Trotta, *Acoustic Sensing for Safety Automotive Applications*, In: Proc The 2nd International Conference on Sensing Technology, 2007, New Zealand.

[8] B. Van Veen, R. Roberts, *A Framework for Beamforming Structures*, IEEE Transactions on Acoustics, Speech, and Signal Processing, 35 (4): 584 – 586, 1987.

[9] P. Vergallo, A. Lay-Ekuakille, *Brain Source Localization: A New Method based on Music Algorithm and Spatial Sparsity*, Rev.SCi.Instrum., vol.84, 085117,2013.

[10] R.M. Cooke D. Kurowicka, *Conditional and partial correlation for graphical uncertainty models*, in Recent Advances in Reldiability Theory, pages 259–276, Birkhauser, Boston 2000.

[11] A. Lay-Ekuakille, P. Vergallo, D. Saracino, A. Trotta, *Optimizing and Post Processing of a Smart Beamformer for Obstacle Retrieval*, IEEE Sensors Journal, vol.12, issue 5, pp.1294-1299, 2012.

[12] E. T.Aung, S. S. Yi Mon, *Performance Comparison of DOA Estimation Algorithms or Smart Antenna*, International Journal of Electronics and Computer Science Engineering, vol.3, n.2, pp.167-174.